The Astrophysical Journal, 749:35 (13pp), 2012 April 10 doi:10.1088/0004-637X/749/1/35

STELLAR LIFETIME AND ULTRAVIOLET PROPERTIES OF THE OLD METAL-RICH GALACTIC OPEN CLUSTER NGC 6791: A PATHWAY TO UNDERSTAND THE ULTRAVIOLET UPTURN OF ELLIPTICAL GALAXIES*

Alberto Buzzoni[1], Emanuele Bertone[2], Giovanni Carraro[3,5], and Lucio Buson[4]
[1] INAF-Osservatorio Astronomico di Bologna, Via Ranzani 1, 40127 Bologna, Italy; alberto.buzzoni@oabo.inaf.it
[2] INAOE-Instituto Nacional de Astrofísica Óptica y Electrónica, Luis Enrique Erro 1, 72840 Tonantzintla, Puebla, Mexico
[3] ESO-European Southern Observatory, Alonso de Cordova 3107, Casilla 19001, Santiago 19, Chile
[4] INAF-Osservatorio Astronomico di Padova, Vicolo Osservatorio 5, 35122 Padova, Italy
Received 2011 September 20; accepted 2012 January 31; published 2012 March 20

ABSTRACT

The evolutionary properties of the old metal-rich Galactic open cluster NGC 6791 are assessed based on deep *UB* photometry and Two Micron All Sky Survey *JK* data. For the 4739 stars in the cluster, bolometric luminosity and effective temperature have been derived from theoretical $(U-B)$ and $(J-K)$ color fitting. The derived H-R diagram has been matched with the Uvblue grid of synthetic stellar spectra to obtain the integrated spectral energy distribution (SED) of the system, together with a full set of UV (Fanelli) and optical (Lick) narrowband indices. The total bolometric magnitude of NGC 6791 is $M_{6791}^{\rm bol} = -6.29$, with a color $(B-V)_{6791} = 0.97$. The cluster appears to be a fairly good proxy of standard elliptical galaxies, although with significantly bluer infrared colors, a shallower 4000 Å Balmer break, and a lower Mg_2 index. The confirmed presence of a dozen hot stars along their extreme horizontal-branch evolution leads the cluster SED to consistently match the properties of the most active UV-upturn galaxies, with $1.7\% \pm 0.4\%$ of the total bolometric luminosity emitted shortward of 2500 Å. The cluster helium abundance results in $Y_{6791} = 0.30 \pm 0.04$, while the post-main-sequence (PMS) implied stellar lifetime from star number counts fairly agrees with the theoretical expectations from both the Padova and Basti stellar tracks. A PMS fuel consumption of $0.43 \pm 0.01\ M_\odot$ is found for NGC 6791 stars, in close agreement with the estimated mass of cluster He-rich white dwarfs. Such a tight figure may lead one to suspect that a fraction of the cluster stellar population does not actually reach the minimum mass required to effectively ignite He in the stellar core.

Key words: galaxies: elliptical and lenticular, cD – galaxies: evolution – open clusters and associations: individual (NGC 6791) – stars: evolution – ultraviolet: galaxies

Online-only material: color figures

1. INTRODUCTION

As a natural marker of the hot stellar component, the study of the ultraviolet (UV) properties of galaxies and smaller star clusters provides us with an important piece of information to more deeply constrain the overall evolutionary status of a stellar aggregate as a whole.

While the implied presence of O-B stars hotter than 30,000–40,000 K is a quite standard condition for any young and/or star-forming system, as in spiral and irregular galaxies (Code & Welch 1982), things are much more puzzling when facing the UV-enhanced luminosity as sometimes observed in the spectral energy distribution (SED) of old quiescent elliptical galaxies. Although within a wide range of strength, the abrupt rise in the UV emission of ellipticals and spiral bulges shortward of 2000 Å, known since the 1980s as the "UV-upturn" phenomenon (Code & Welch 1979; Bertola et al. 1982), seems to characterize the stellar population in old metal-rich environments. This poses a crucial constraint on stellar evolution theory in order to place this effect into a convenient theoretical framework.

Among the different UV sources one can find in any old stellar population (see, e.g., Yi & Yoon 2004, for an updated review), hot post-asymptotic-giant-branch (post-AGB or PAGB) and extreme horizontal-branch (EHB) stars stand out as main contributors to short-wavelength emission. Depending on the core/envelope mass ratio (M_c/M_e), evolution of low-mass $(M \lesssim 2\ M_\odot)$ stars actually heads to the final white dwarf (WD) stage either through a full completion of the AGB phase and the subsequent planetary-nebula event (hot-PAGB evolution, see, e.g., Paczyński 1970; Iben & Renzini 1983), or by skipping partially or in toto any AGB evolution (Greggio & Renzini 1990). EHB stars are the natural outcome in the latter case, being on route toward the WD cooling sequence after completing the horizontal-branch (HB) evolution (Dorman et al. 1995; D'Cruz et al. 1996). In both cases, stellar structure is characterized by a shallow external envelope that lets the hot H-burning shell "emerge" close to the stellar surface, thus moving stars toward the high-temperature region of the H-R diagram.

In the color–magnitude (c-m) diagrams of a few globular clusters—ω Cen (D'Cruz et al. 2000) and NGC 2808 (Harris 1974; Castellani et al. 2006b) are good examples in this sense—EHB stars appear to clump at the hot-temperature edge of the HB being classified, from the spectroscopic point of view, as hot subdwarfs (sdB). Spectroscopy (Brown et al. 1997) and imaging (Brown et al. 2000) of resolved c-m diagrams for stellar populations in local galaxies, like M32, seem to point to these stars as the main reason for the UV upturn, providing that some (unknown) critical threshold in [Fe/H] is exceeded to trigger the phenomenon (e.g., Greggio & Renzini 1990; Bressan et al. 1994; Buzzoni 1995a, 2007; Dorman et al. 1995).

* Based on observations carried out at the Italian Telescopio Nazionale Galileo, operated by INAF at the Roque de los Muchachos Observatory (La Palma, Spain).
[5] On leave from Dip. di Astronomia, Universitá di Padova, Padova, Italy.

Although metallicity might be the leading parameter in the game, the exact physical mechanisms at work still lack any firm observational confirmation as photometry of evolved UV-bright stars in external galaxies are still confined to the relevant case of M31 and its satellite system (e.g., Bertola et al. 1995; Brown et al. 1998, 2000), and no suitable spectroscopy for single stars is available to date. The study of old metal-rich open clusters in the Galaxy may provide important clues in this regard. Although over a much reduced mass scale, open clusters may prove, in fact, to be an effective proxy to constrain the nature of the again-emerging UV in elliptical galaxies and spiral bulges.

In this framework NGC 6791 perhaps plays a central role, being, with its ∼4000 $M_\odot$ (Kinman 1965; Kaluzny & Udalski 1992), among the most massive and populated open clusters in our Galaxy. Its old age, about 8 Gyr, has recently been confirmed by Chaboyer et al. (1999), Anthony-Twarog et al. (2007), and Grundahl et al. (2008), relying on CCD photometry, while extensive high-resolution spectroscopy of member stars (Peterson & Green 1998; Carraro et al. 2006; Origlia et al. 2006; Gratton et al. 2006; Boesgaard et al. 2009) points to a supersolar metallicity (i.e., [Fe/H] $\sim +0.4 \pm 0.1$). Located about 4 kpc away (Carraro et al. 1999, 2006; Carney et al. 2005) in an oscillating orbit that periodically brings it closer to the bulge of the Milky Way (Bedin et al. 2006; Wu et al. 2009), NGC 6791 stands out as a sort of backyard "Rosetta Stone" to assess the UV emission of more distant ellipticals.

This match is even more reinforced by the truly peculiar hot-HB content of this cluster, with a sizable fraction of sdB/O stars, as first detected by Kaluzny & Udalski (1992) and Kaluzny & Rucinski (1995). On the basis of ground and space-borne (Ultraviolet Imaging Telescope and *Hubble Space Telescope*) UV observations (Yong & Demarque 2000; Liebert et al. 1994; Landsman et al. 1998), these hot sources have then been interpreted as EHB stars with $T_{\rm eff} \sim$ 24–32,000 K. Some hints for the presence of a composite stellar population in NGC 6791 recently came from Twarog et al. (2011), who reported a significant color shift in the main-sequence (MS) location along the cluster radius. This feature may lead to an age ∼1 Gyr older in the core region compared to cluster periphery, although an alternative explanation in terms of a reddening gradient may not be firmly excluded (Platais et al. 2011).

Facing the relevance of NGC 6791 as a potentially effective proxy of UV-upturn ellipticals, in this paper we present the results of an application of population synthesis techniques to further explore the evolutionary lifetime of the cluster stellar population and the integrated UV properties of the system as a whole. For our task we take advantage of a new set of deep *UB* CCD photometry, resolving stars down to $B \sim 22$, complemented at bright luminosity by the Two Micron All Sky Survey (2MASS) IR observations. This observing data set is briefly described in Section 2, referring the reader to an accompanying paper (L. M. Buson et al. 2012, Paper II, in preparation) for more details. By calibrating the apparent color of our stars with a set of theoretical models we have been able, in Section 3, to convert the c-m diagram of the cluster into the H-R fundamental plane of bolometric luminosity and effective temperature. This allowed us to single out and study in fairly good detail the hot stellar component of the cluster, and led to the integrated SED of the whole aggregate, by summing up the spectrophotometric contribution of each star (Section 4). By relying on the synthetic broadband colors and narrowband UV and optical spectrophotometric indices, we assess in Section 5 the problem of how close NGC 6791 resembles the case of UV-upturn elliptical galaxies. Finally, a careful match of the star number counts across the cluster H-R diagram and the theoretical prescriptions of the so-called fuel consumption theorem (FCT) of Renzini & Buzzoni (1986) led us to derive, in Section 6, the implied stellar lifetime along the different evolutionary branches of the diagram, together with an estimate of the corresponding energetic constraints from the consumed nuclear fuel inside stars. A number of interesting implications on the distinctive evolutionary properties of the cluster are therefore discussed in this section, and further expanded in the final summary of our conclusions in Section 7.

2. OBSERVING DATABASE AND CLUSTER SELECTION

A set of deep CCD U, B imagery of NGC 6791 has been collected at the 3.6 m Telescopio Nazionale Galileo (TNG) of La Palma (Spain) from the three nights of 2003 July 29–31. The cluster field has been sampled by stacking four (partially overlapping) 9.′4 × 9.′4 quadrants of the sky taken with the LRS FOSC camera equipped with a 2048 × 2048 back-illuminated E2V CCD. This setup provided a plate scale of 0.″275 pixel^{-1} across a total field of 17.′0 × 17.′0 (roughly 20 × 20 pc across, at the cluster distance). Exposure time for the U observations was 1200 s, while B frames were taken with 300 s. A standard photometric reduction of the images was carried out, relying on Landolt (1992) reference fields, and by matching a supplementary set of 16 cluster stars in common with the photoelectric observations of Montgomery et al. (1994).

Data have been reduced with the IRAF[6] packages CCDRED, DAOPHOT, ALLSTAR, and PHOTCAL using the point-spread function method (Stetson 1987). This led to a photometric catalog with 7831 entries of stars down to $B \sim 22$ mag with measured $U - B$ color. For the reader's convenience, a detailed discussion of this database is deferred to Paper II, only focusing here on the application of the photometric catalog to our cluster spectral synthesis procedure.

For its low Galactic latitude $(l, b) = (70^\circ, +10.^\circ9)$, NGC 6791 is heavily embedded into a Galaxy disk. This is evident at first glance from the resulting c-m diagram of the sky region surrounding the cluster (see Figure 1, and even more clearly Kaluzny & Rucinski 1995). A comparison with synthetic c-m diagrams of the same region, as from the Girardi et al. (2005) Galactic model (see Paper II for details), makes clear that a major contamination along the cluster sightline comes from bright A-F stars belonging to the thick-disk stellar component, while a negligible contribution from stars of later spectral type has to be expected, especially as foreground interlopers. This provides us with a simple diagnostic scheme as one can imagine to (mostly) pick up the bona fide cluster stellar population by rejecting field A-F stars in a $-0.4 \lesssim (U - B) \lesssim +0.25$ color strip (see, e.g., Johnson 1966 for the relevant fiducial colors) and all "redder" (i.e., later type) objects fainter than the fiducial MS locus of the cluster, as sketched in Figure 1.

With these magnitude/color cuts, we are eventually left with a total of 5202 stars in our *UB* catalog. After a reddening correction, assuming a color excess $E(B - V) = 0.125$ or $E(U - B) = 0.09$ from Twarog et al. (2009) this bona fide star sample provides an integrated magnitude and color of $[B_o, (U - B)_o] = [8.77, 0.56]$.

Being especially focused on the study of the hot stellar component in the cluster, our *UB* imagery is of course not well

[6] IRAF is distributed by NOAO, which is operated by AURA under cooperative agreement with the NSF.

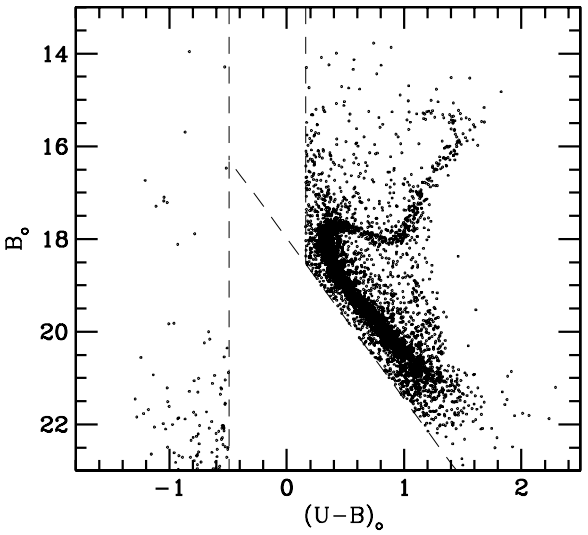

Figure 1. Observed B vs. $(U-B)$ c-m diagram of NGC 6791, according to our deep TNG photometry. Magnitude and color have been corrected for reddening according to Twarog et al. (2009). To statistically pick up the genuine cluster stellar population, we applied to the plot a selection in the observed (i.e., non-dereddened) color domain by rejecting as possible field interlopers all the stars included in a $-0.4 \lesssim (U-B) \lesssim +0.25$ color strip plus those objects lying below the MS locus, as sketched in the diagram.

suited to also match the cool red giant stars. To a more accurate check of the resulting c-m diagram, in fact, most of these stars suffered from poor photometry as their exceedingly red colors often required some prudent extrapolation of our photometric solution. In addition, the reddest stars were sometimes barely detectable in the U frames or conversely became partly saturated in B. For this reason, the bright stellar sample in the cluster field (including basically all the red giant branch (RGB)+AGB stars for $B \gtrsim 15$) has been directly assessed through the infrared observations of the 2MASS survey (Skrutskie et al. 2006).

A selection of all the 2MASS stellar candidates across our field with color $(J-K) \geqslant 0.35$ (which is consistent with or redder than the cluster turnoff point) provided 94 stars, of which 61 objects were also caught by our *UB* survey, though in a few cases (three stars) as saturated objects. The remaining 33 objects were actually not comprised in our *UB* catalog being all bright stars sampling the reddest tail in the overall color distribution.

3. THE FUNDAMENTAL PARAMETERS OF CLUSTER STARS

In order to create a self-consistent spectral synthesis of the cluster stellar population, apparent magnitudes and colors of member stars have to be converted to the fundamental physical plane of the H-R diagram to safely derive for each star its intrinsic parameters (namely bolometric luminosity, effective temperature, and surface gravity). An iterative algorithm has been set up in this regard, with the help of the UVBLUE synthetic library of stellar spectra (Rodríguez-Merino et al. 2005), computed for [Fe/H] = +0.4 and with the Castelli & Kurucz (2003) revised chemical opacities, as shown in Figure 2.

To avoid spurious transformations in consequence of high color uncertainty of faint objects, we only analyzed stars in our bona fide sample brighter than $B = 21.5$, namely about 3.5 mag below the turnoff point. These total 4706 entries in the *UB* catalog, of which 61 objects overlap the 2MASS sample. For each star we proceeded first by fixing a reference value for surface gravity, namely $\log g = 3$. With this value and the

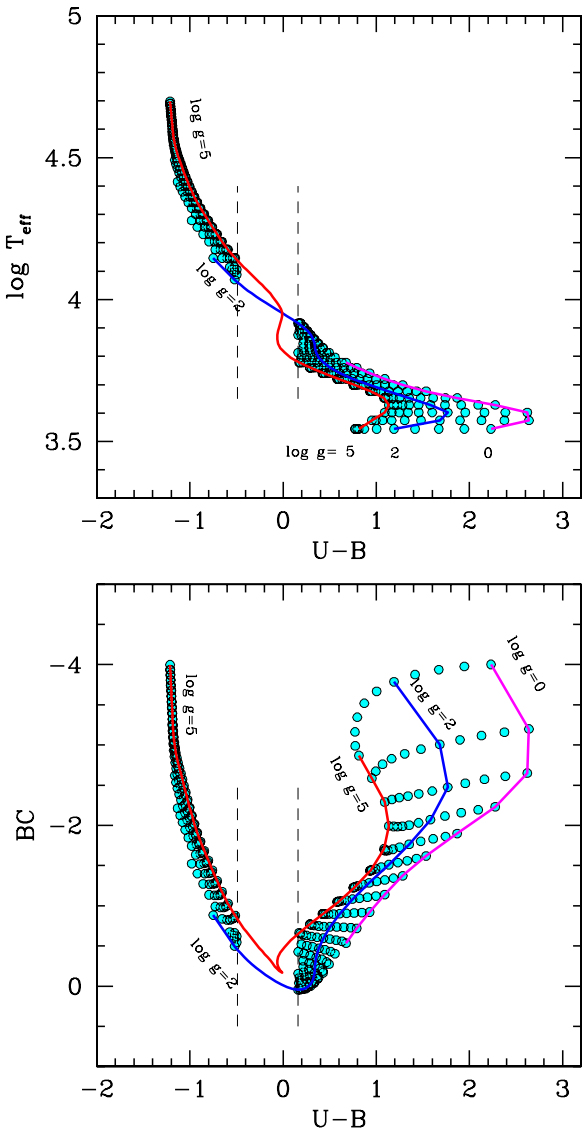

Figure 2. Theoretical relationship between $(U-B)$ color, effective temperature (upper panel), and B-band bolometric correction (lower panel) for stars with [Fe/H] = +0.4, according to the UVBLUE grid of synthetic stellar spectra (Rodríguez-Merino et al. 2005) in its updated version with the Castelli & Kurucz (2003) revised chemical opacities. The model sequences for fixed values of surface gravity, namely $\log g = 0, 2$ (giants), and 5 (dwarfs), are singled out and labeled on the plots for the reader's reference. The assumed "zone of avoidance" for field interlopers has been marked in each grid.

(A color version of this figure is available in the online journal.)

(dereddened) $(U-B)$ color of the star, we then entered the two panels of Figure 2, deriving a guess value for $\log T_{\rm eff}$ and the B-band bolometric correction, BC = Bol − B. With the help of BC, and once accounting for the reddening and distance modules, the latter being $(m-M) = 13.07$ as from Twarog et al. (2009), the B apparent magnitude can eventually be converted to $\log L/L_\odot$. At this point, a self-consistency check must hold as, by definition,

$$\log(L/L_\odot) = 2\,\log(R/R_\odot) + 4\,\log(T_{\rm eff}/T_\odot). \qquad (1)$$

As the stellar radius R is tied to g through $g = GM/R^2$, then Equation (1) can easily be rewritten in terms of stellar surface gravity as

$$\log(L/L_\odot) = \log(M/M_\odot) - \log(g/g_\odot) + 4\log(T_{\rm eff}/T_\odot), \quad (2)$$

where we assume $\log g_\odot = 4.45$ in cgs units and $T_\odot = 5780$ K for the Sun. Note that Equation (2) only weakly depends on the exact value of the stellar mass (M). For example, even a factor-of-two uncertainty on M would only reflect into a $\Delta \log g \sim \pm 0.3$ uncertainty, which is safely within the sampling step of the UVBLUE model grid (i.e., $\Delta \log g = 0.5$ dex). Considering the estimated age for NGC 6791 and the implied turnoff mass, we could conservatively set $M = 1\,M_\odot$ with no relevant impact on our conclusions.

At this point, by entering Equation (2) with the guess values for $\log T_{\rm eff}$ and $\log L$, we get back a refined ("predicted") estimate for $\log g$ to be used for a new iteration, such as

$$\log g_{\rm pred} = 4 \log T_{\rm eff} - \log(L/L_\odot) - 10.60. \quad (3)$$

The iterative procedure has been carried on for each entry of our bona fide catalog until the "predicted" $\log g$ matches, within ± 0.25 dex, the previous guess value. Accordingly, this also left us with the final values for $\log L$ and $\log T_{\rm eff}$. It could be verified that a solution is quickly achieved in a couple of iterations or so, providing that the star is located in the sampled domain of the UVBLUE models. This has actually always be the case, except for the little bunch of WD stars easily recognized in the c-m diagram of Figure 1, fainter than $B \gtrsim +20$ and with negative $(U-B)$ colors. Their gravity is far larger ($\log g \sim 6$–7) than the UVBLUE domain so that they have to be forcedly approximated within the theoretical grid with $\log g = 5$ models.

A different procedure has been applied, on the contrary, for the 94 stars included in the 2MASS sample. For them we relied on the accurate bolometric calibration by Buzzoni et al. (2010), who accounted for NGC 6791 red giants in their analysis. According to the (dereddened) $(J-K)$ color, we obtain for our cluster the following transformation equations:[7]

$$\begin{cases} \log T_{\rm eff} = -0.248\,(J-K) + 3.82 \\ \quad [\rho, \sigma] = [0.97, 0.012\,\text{dex}] \\ \\ ({\rm Bol} - K) = 1.594\,(J-K) + 1.13 \\ \quad [\rho, \sigma] = \left[0.98, 0.04\,\text{mag}\right]. \end{cases} \quad (4)$$

A comparison of the two calibration procedures for our 58 2MASS stars with available $(J-K)$ and unsaturated $(U-B)$ color confirmed that effective temperature is derived within an internal accuracy of ~6% (namely $\langle \Delta \log T_{\rm eff} \rangle = +0.011 \pm 0.027$ dex, in the sense "$UB-JK$"), while the bolometric magnitude scale is reproduced within a $\langle \Delta {\rm Bol} \rangle = -0.12 \pm 0.22$ mag accuracy.

In total, bolometric luminosity and effective temperature have been secured for 4739 stars. 4645 entries come from the *UB* bona fide sample and 94 stars from the 2MASS database.[8]

3.1. The Cluster H-R Diagram

The resulting H-R diagram from our iterative conversion of the B versus $(U-B)$ plot of Figure 1, plus the bright 2MASS extension, is displayed in Figure 3. As a reference guideline, we superposed to the stellar distribution two isochrones from the Padova database (Bertelli et al. 2008), for $t = 6$ and 8 Gyr and $(Z, Y) = (0.04, 0.34)$, closely matching the cluster metallicity. The fairly good agreement confirms the reliability

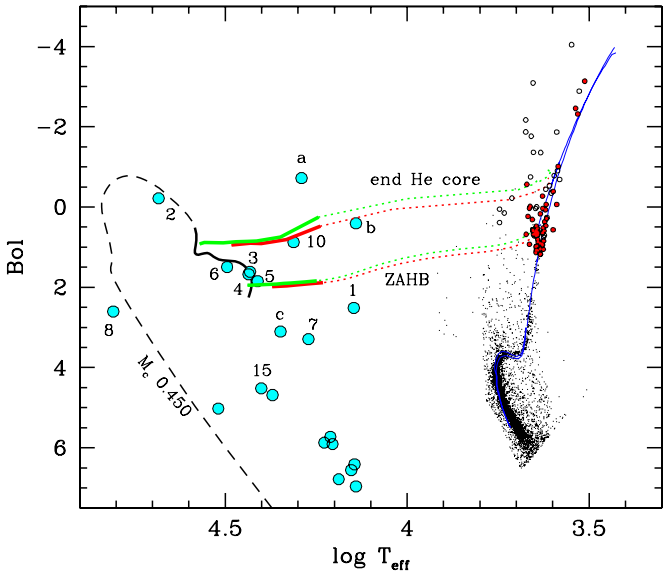

Figure 3. Derived H-R diagram of NGC 6791. Big (blue) dots mark the hot stellar component with $T_{\rm eff} \gtrsim 10{,}000$ K. When available, stars are labeled with their ID number from the Kaluzny & Udalski (1992) catalog. Three new stars, consistent with hot-HB evolution, appear in our survey and are labeled with "a," "b," and "c" in the plot. Small dots in the red giant region of the diagram indicate the 94 2MASS stars that integrated our *UB* photometry, as discussed in the text. Of these, the 61 stars in common with the *UB* sample appear as (red) solid dots. The theoretical isochrones from the PADOVA database (Bertelli et al. 2008) for $(Z, Y) = (0.04, 0.34)$ and $t = 6$ and 8 Gyr are overplotted to the data, together with the expected HB evolutionary strip between the ZAHB locus as a lower edge and the He core exhaustion locus as an upper envelope. Calculations for HB models are from the BASTI database (Pietrinferni et al. 2007) for a $(Z, Y) = (0.04, 0.30)$ chemical mix with solar-scaled (red curve, from Pietrinferni et al. 2004) and α-enhanced (green curve, from Pietrinferni et al. 2006) metal partition. The case of a $0.45\,M_\odot$ star evolving as an EHB (and AGB-*manqué*) object is also displayed in some detail (thick black solid line), according to D'Cruz et al. (1996) for [Fe/H] = +0.37. See the text for a discussion.

(A color version of this figure is available in the online journal.)

of our transformation procedure. The turnoff point appears to have an effective temperature $T_{\rm eff} \simeq 5700 \pm 50$ K, consistent with a spectral type G5 (Johnson 1966).

Just a glance at the figure makes evident one outstanding feature of NGC 6791's stellar distribution, with a marked deficiency of bright red giants, surmounting the luminosity level of the red HB clump. This scanty population of bright cool stars (assumed to include both the bright tail of RGB evolution and the full AGB phase), compared for instance with the HB population, is in fact an established feature of NGC 6791 (Kalirai et al. 2007), also widely recognized in other observing sets taken in different photometric bands (see, for instance, the c-m diagram of Montgomery et al. 1994; Kaluzny & Rucinski 1995; Stetson et al. 2003; Platais et al. 2011). These arguments led Kalirai et al. (2007) to envisage a sort of physical link, essentially driven by enhanced stellar mass loss, between the peculiar RGB morphology of NGC 6791 and a prevailing presence of low-mass ($\langle m_{\rm WD} \rangle = 0.43 \pm 0.06\,M_\odot$) He-rich WDs, a feature that might call for the anticipated completion of RGB evolution, missing in some cases even the canonical He-flash event.

Although within the large uncertainties due to the low statistics and the intervening effect of field contamination, we think that even a raw estimate of the HB versus bright RGB+AGB relative number counts can offer an interesting alternative interpretation, being that the ratio is strongly modulated by the helium abundance of the cluster stellar population. As a

[7] In addition to the luminosity and temperature estimates from Equation (4), a measure of surface gravity for these stars can be obtained via Equation (3).

[8] Note that for the 61 stars with available *UB* and *JK* photometry, the latter calibration was eventually retained for our analysis.

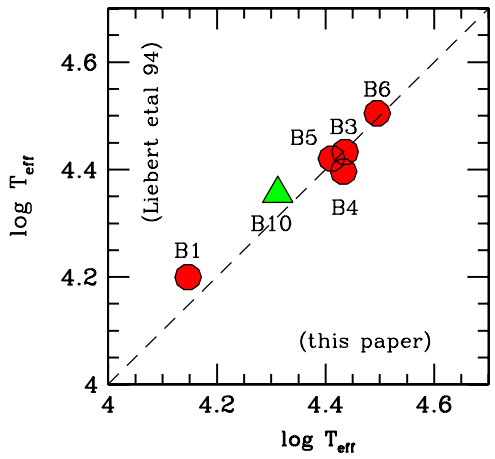

Figure 4. Liebert et al. (1994) temperature scale from high-resolution spectroscopy compared with our $(U - B)$-based calibration for the five hot stars in the Kaluzny & Udalski (1992) list, as labeled (big dots). One more star in the list (B10) has been made available from the Landsman et al. (1998) spectroscopy and has been added to the plot (big triangle). Spectroscopic temperature estimates are confidently reproduced by our photometric calibration within a ±7% (1σ) relative scatter.

(A color version of this figure is available in the online journal.)

well-established result (Iben 1968), in fact, stellar evolution theory tends to predict a quicker RGB evolution at bright luminosity with increasing helium abundance. Consequently, a larger $R = N_{\rm HB}/N_{\rm RGB}$ ratio has to be expected in helium-rich stellar systems. As we will show in more detail in Section 7, this might actually be the case for NGC 6791.

3.2. The Hot Stellar Component

The H-R diagram of Figure 3 allows us to make a clean assessment of the hot stellar component in the cluster. This recognition is actually favored by the sensitivity of the $(U - B)$ color to the temperature range of B stars, hotter than $T_{\rm eff} \sim 10{,}000$, as shown in Figure 2. In particular, the HB morphology can be accurately traced by our calibration, although a few possible A-type member stars may have been missed according to our color selection, as explained in Section 2.

A straight comparison of our data can be performed in Figure 3 with the theoretical zero-age horizontal branch (ZAHB) and the upper envelope tracing the end of the core He-burning stage, according to the BASTI model database (Pietrinferni et al. 2007). A standard solar-scaled chemical composition has been assumed, as from Pietrinferni et al. (2004), with $(Z, Y) = (0.04, 0.30)$, together with the α-enhanced case (Pietrinferni et al. 2006). For both model sets we singled out with solid tick lines in the figure the locus of $M \leqslant 0.48\,M_{\odot}$ stars which, for this metallicity, identify the EHB objects. At least six stars in our sample seem to match this constraint. They are all comprised in the list of UV-bright stars proposed by Kaluzny & Udalski (1992), with ID code B02, B03, B04, B05, B06, and B10 (see Paper II for a detailed discussion). Most of them have been spectroscopically characterized by Liebert et al. (1994) and Landsman et al. (1998), leading to an accurate temperature classification. As an important cross-check of our transformation procedure, we compared in Figure 4 our temperature scale obtained from the $(U - B)$ color and the corresponding estimate by Liebert et al. (1994) from the spectral fit of the Balmer absorption lines with synthetic high-resolution spectra. The agreement is most encouraging, with a relative scatter of ±7% (at 1σ level), in the inferred values of $T_{\rm eff}$ with the two methods.

A closer inspection of Figure 3 reveals, however, that a few other stars (three new ones marked with the letters "a," "b," and "c" in the plot plus the Kaluzny object B08) may still be viable hot-HB members owing to the photometric uncertainty that somewhat scatters the point distribution in the diagram. Two more objects in this region (namely stars B01 and B07 in the Kaluzny & Udalski 1992 original list) were first claimed to be field stars by Liebert's (1994) spectroscopy, but they now seem to be re-admitted as definite cluster members based on the astrometric analysis of Platais et al. (2011).[9] These alleged cases warn, however, of the possible amount of contamination by field interlopers.

4. CLUSTER SPECTRAL SYNTHESIS

As a final, and possibly most instructive exercise, we rely on the derived set of $(\log L, \log T_{\rm eff}, \log g)$ fundamental parameters of our bona fide cluster sample to sum up the expected spectrophotometric contribution of each star such as to obtain the integrated SED of the cluster as a whole.

This task has been first carried out at a low spectral resolution, especially addressing the optical/infrared wavelength range. We made use, in this regard, of the original ATLAS9 grid of Kurucz's (1993) synthetic stellar spectra, sampling wavelength at 25–50 Å steps. In addition, to gain a better view of the UV distinctive properties of the cluster stellar population, we also carried out a high-resolution (2 Å FWHM) spectral synthesis between 870 and 3300 Å by matching stars with the appropriate UVBLUE spectral grid. As a general procedure in both cases, each star has been located within the relevant grid according to its fundamental parameters, and the corresponding synthetic SED has been attached to it in order to normalize flux density such as to match the value of the bolometric luminosity. By summing up all 4739 entries brighter than $B = 21.5$, we eventually led to an estimate of the integrated SED of NGC 6791. Our results are displayed in Figure 5.

The synthetic SED opens a number of interesting applications. Besides computing broadband colors along the entire wavelength range, we could also estimate narrowband spectrophotometric indices, either via direct integration on the synthetic spectrum or by means of the so-called fitting-function procedure (Buzzoni et al. 1992; Worthey et al. 1994). As for the first case, the Fanelli et al. (1990) mid-UV indices have been obtained, to degrade our spectral resolution to 6 Å (FWHM) in order to match the standard system definition (see also Chavez et al. 2007, for details). In addition, a relevant subset of Lick narrowband indices has been obtained by relying on two independent schemes of index fitting functions, according to Buzzoni et al. (1992, 1994) and Worthey et al. (1994). We therefore dealt with the integrated strength of the Hβ Balmer line, the popular magnesium absorption features (Mg_2 and Mg_b indices), and three recognized Fe I blends around 5000 Å (Fe5015, Fe5270, and Fe5335 indices). A direct assessment of the 4000 Å Balmer break has been possible, as well, through the two indices Δ, originally defined in mag scale by Brodie & Hanes (1986) and Brodie & Huchra (1990), and $D4000$, in terms of flux ratio as from Bruzual (1983) (see also Hamilton 1985; Gorgas et al. 1999).

[9] A further star, B10, is questioned as a field member by Platais et al. (2011), but see Paper II.

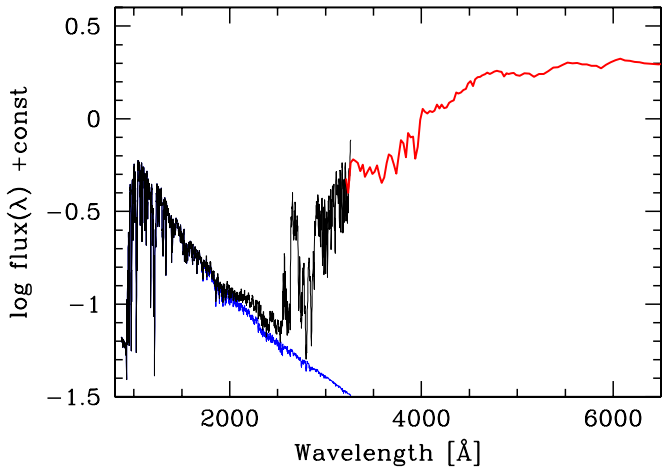

Figure 5. Synthetic SED of NGC 6791. The integrated spectrum is obtained by summing up the contribution of our bona fide star sample of 4739 entries. Mid-UV ($\lambda \lesssim 3200$ Å) spectral synthesis has been carried out at high resolution (2 Å FWHM) by attaching each star to the corresponding UVBLUE synthetic spectrum with the same fundamental parameters (black line). The same procedure has been adopted at a longer wavelength (red line) by matching the Kurucz's (1993) ATLAS9 library at low resolution (~25 Å). The selective contribution of hot ($T_{\rm eff} \geqslant 10{,}000$ K) is singled out (blue line) showing that these stars are the prevailing contributors to the striking UV upturn in this SED. According to our estimate (see Equation (6)) this feature collects about 1.7%±0.4% of the total bolometric luminosity of the cluster.

(A color version of this figure is available in the online journal.)

For the reader's convenience, the full set of broadband synthetic colors for NGC 6791, including the Johnson/Cousins, Gunn, *GALEX* photometric systems and Balmer-break indicators, is summarized in Table 1. The narrowband spectrophotometric indices are collected, instead, in Table 2.

A first direct estimate of the integrated color of NGC 6791 has been attempted by Kinman (1965), who probed the central region of the cluster obtaining (after correction to our reddening scale) $(B-V)_o^{\rm tot} = 0.96$, in perfect agreement with our synthesis output. An isochrone approximation of the same data, and with the same reddening offset, led Xin & Deng (2005) to obtain $(B-V)_o^{\rm tot} = 1.07$, while Lata et al. (2002), from a coarser set of observations, propose $(B-V)_o^{\rm tot} = 1.1 \pm 0.2$ for the cluster. Both these sources, however, tend to be biased against bluer objects. Based on the Kaluzny & Rucinski (1995) and Stetson et al. (2003) *BV* database, we carried out different experiments by summing up stars in each catalog after cleaning the field-stars according to the color selection scheme of Section 2. A more realistic figure, still adopting our $E(B-V)$ color excess, can be envisaged for the integrated color in the range $(B-V)_o^{\rm tot} \simeq 0.95 \pm 0.03$ for Kaluzny & Rucinski (1995) and $(B-V)_o^{\rm tot} \simeq 1.00 \pm 0.02$ for Stetson et al. (2003).

According to the H-R transformation, the bolometric emission of the integrated SED of Figure 5 amounts to $M_o^{\rm bol} = -6.29$, which implies a total luminosity of the sampled cluster population of

$$L_{6791}^{\rm bol} = 10^{-0.4\,(M_o^{\rm bol} - M_\odot^{\rm bol})} = 25{,}350\,L_\odot, \qquad (5)$$

assuming $M_\odot^{\rm bol} = 4.72$ from Portinari et al. (2004). According to our total *V*-band magnitude $M_{\rm tot}^V = -5.60$, cluster luminosity results are about a factor of two brighter than Kinman's (1965) original output (once converted to our reddening scale and distance modulus), but one has to consider, in this regard, that we are sampling a wider field by a factor of four. Again, with our prescriptions for distance and reddening correction, the previous experiments with the Kaluzny & Rucinski (1995) and Stetson et al. (2003) *BV* stellar sets provided us with a value of $M_{\rm tot}^V = -5.95 \pm 0.07$ and -5.62 ± 0.03, respectively, in

Table 1
Broadband Magnitude and Color Properties from Spectral Synthesis of NGC 6791[a] Compared to Standard Elliptical Galaxies

	NGC 6791	Ellipticals[b]	System Ref.
$M_{\rm bol}$	−6.29	...	...
Bol − *V*	−0.69	...	Johnson
$U-B$	0.60	0.56	”
$B-V$	0.97	0.97	”
$V-R$	0.86	0.86	”
$V-I$	1.50	1.63	”
$V-J$	2.08	2.35	”
$V-H$	2.74	3.05	”
$V-K$	2.90	3.28	”
$V-R_c$	0.60	0.61	Johnson/Cousins
$V-I_c$	1.18	1.31	”
M_g	−5.38	...	Gunn
$g-r$	0.45	0.40	”
$g-i$	0.67	0.70	”
$g-z$	0.79	0.96	”
$1550-V$	2.44 ± 0.25	>2.17 ± 0.15	Burstein et al. (1988)
FUV − *V*	5.22 ± 0.25	>4.95 ± 0.15	*GALEX*[c]
NUV − *V*	5.01 ± 0.25	>4.56 ± 0.15	”
Balmer-break indices:			
Δ	0.36	...	Brodie & Hanes (1986)
*D*4000	1.82	2.16 ± 0.24	Bruzual (1983)[d]

Notes.
[a] Reddening and distance modulus according to Twarog et al. (2009); the error bar for the UV colors from Poissonian number fluctuation of bright hot stars of Figure 3.
[b] Johnson colors are from Yoshii & Takahara (1988); Cousins and Gunn colors from Fukugita et al. (1995); $(1550-V)$, and *GALEX* average colors for the four strongest UV-upturn galaxies in Figure 7; Balmer-break index *D*4000 from Hamilton (1985).
[c] *GALEX* colors in AB magnitudes.
[d] Index value as a flux ratio.

Table 2
Mid-UV, Balmer-break, and Selected Lick Spectrophotometric Indices of NGC 6791

Mid-UV Indices[a]		Lick Indices		
Fe II 2332	0.123	Hβ	1.92	Å
Fe II 2402	0.145	Fe5015	7.44	Å
BL 2538	0.374	Mg_2	0.246	mag
Fe II 2609	1.328	Mg_b	4.28	Å
BL 2720	0.410	Fe5270	3.51	Å
BL 2740	0.523	Fe5335	3.16	Å
Mg II 2800	0.668			
Mg I 2852	0.700			
Mg wide	0.343			
Fe I 3000	0.286			
BL 3096	0.170			
2110/2570	0.132			
2600–3000	0.969			
2609/2660	1.328			
2828/2921	0.778			
S2850	1.277			
S2850L	1.447			

Note. [a] Index values in mag, as defined by Fanelli et al. (1990) and Chavez et al. (2007).

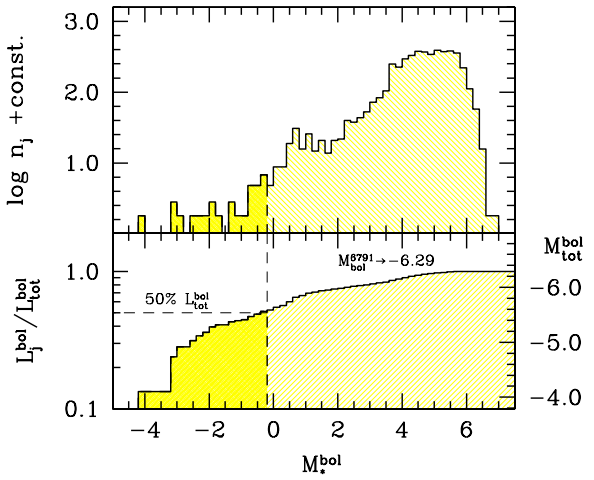

Figure 6. Upper panel: the bolometric luminosity function of the NGC 6791 stellar population according to the c-m diagram of Figure 3. Lower panel: the cluster integrated magnitude obtained by summing up stars with increasingly fainter bolometric luminosity. An asymptotic value of $M^{\rm bol}_{\rm tot} = -6.29$ is reached when including all 4739 stars in our sample. Note the outstanding contribution of the few bright stars with a negative value of $M^{\rm bol}_{*}$ (some 30 objects in total), which provide about 50% of cluster total luminosity.

(A color version of this figure is available in the online journal.)

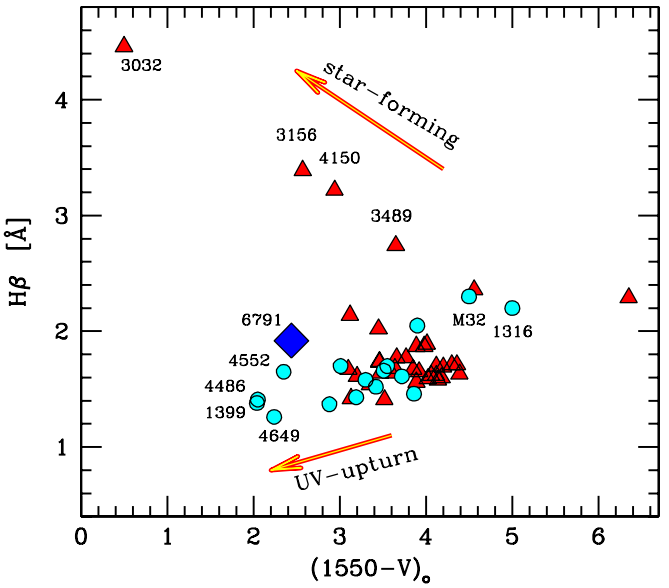

Figure 7. Comparison of the NGC 6791 location in the Hβ index vs. $(1550-V)$ UV color (big rhombus marker, as labeled) is carried out with a set of elliptical galaxies along a range of evolutionary cases. The Bureau et al. (2011) Sauron database of 41 ellipticals with available *GALEX* UV photometry is displayed (triangles) together with the original *IUE* sample of Burstein et al. (1988), as recompiled by Buzzoni & González-Lópezlira (2008) (18 galaxies with available Lick indices; solid dots). Some reference objects are singled out and labeled for better clarity (see text for a discussion). A clear "$>$"-shaped pattern of galaxy distribution is in place, with mildly star-forming systems displaying a stronger ($\gtrsim$2 Å) Hβ index, contrary to UV-upturn galaxies, which supply the same UV emission with a much shallower Hβ absorption. Note the resemblance of NGC 6791 with the case of galaxy NGC 4552.

(A color version of this figure is available in the online journal.)

far better agreement with our prediction once considering the slightly different sampled area.

Although a prevailing fraction of the cluster total luminosity certainly comes from the few bright giant stars in our sample, one may argue that our estimate of $L^{\rm bol}_{6791}$ is a somewhat lower limit as (1) we are missing the contribution of the faintest MS stars and (2) we might be sampling just a fraction of the total cluster, according to our observed field. A preliminary estimate of point (1) can be attempted by relying on the combined analysis of the luminosity function and the cumulative luminosity contribution of the star counts versus absolute stellar luminosity. This is shown in Figure 6. One may guess from the figure that sampling completeness of our luminosity function safely extends down to $M^{\rm bol}_{*} \lesssim +5.5$. Even assuming that star counts steadily increase with the same trend at fainter magnitudes,[10] we verified that the inferred $L^{\rm bol}_{6791}$ value would increase by 15% at most.

Concerning the spatial sampling, as for point (2) of our caveat, we made use of the V data from Stetson et al. (2003), collected over a larger field ($\sim 20' \times 20'$) compared to our observations, to derive an estimate of the lost luminosity fraction. From these data, after fitting the star distribution with a King (1966) profile we obtain a photometric (projected) and tidal radius for the cluster, respectively, of $R_c = 4.75 \pm 0.29$, and $R_t = 20.57 \pm 7.48$ arcmin,[11] in nice agreement with the recent study of Platais et al. (2011). With these shape parameters, according to the V luminosity profile, we estimate that about 95% of cluster luminosity has been effectively collected by our observations.

5. NGC 6791 AS A PROXY OF UV-UPTURN ELLIPTICAL GALAXIES?

Based on the resolved H-R diagram of Figure 3, the contribution of the different stellar evolutionary stages to the integrated SED of the cluster can be easily disaggregated. As an outstanding feature, in this regard, one sees from Figure 5 that the hot stellar component with $T_{\rm eff} \gtrsim 10{,}000$ K is by far the prevailing contributor to the UV luminosity of the cluster shortward of 2500 Å. Actually, these stars are primarily responsible for the striking "UV upturn" in the spectrum of NGC 6791. A close resemblance with the corresponding feature that sometimes marks the SED of elliptical galaxies evidently calls for special analysis of our data in order to assess how confidently we can retain NGC 6791 as a suitable "proxy" of UV-enhanced ellipticals.

The strength of the UV upturn for the cluster is probed in Table 1 by the classical $(1550 - V)$ color, as originally defined by Burstein et al. (1988). A nearly equivalent definition can be obtained in an updated AB mag scale based on the *GALEX* photometric system, as $({\rm FUV} - V) \simeq (1550 - V) + 2.78$ (see, e.g., Neff et al. 2008), as reported in the same table. According to our synthesis output, hot stars supply a total of 430 $L_\odot$ so that the relative contribution of the UV emission to the total bolometric luminosity of the cluster is

$$\frac{L^{\rm UV}_{\rm hot*}}{L^{\rm bol}_{6791}} = \frac{430}{25,\,350} = 0.017 \pm 0.004, \qquad (6)$$

where the error bar has been estimated from the Poissonian number fluctuation of the 12 bright hot stars of Figure 3.

To properly set this figure in the more general extragalactic framework, in Figure 7 we compare the NGC 6791 output with a set of elliptical galaxies spanning a wide range of evolutionary cases. In particular, the original *IUE* sample of Burstein et al. (1988), recently recompiled by Buzzoni & González-Lópezlira (2008; 18 galaxies with available Lick indices), has been

[10] An intrinsic flattening of the luminosity function just fainter than the turnoff point (i.e., $M^{\rm bol}_{*} \simeq +4.0$) is, however, confirmed also by the results of Kaluzny & Rucinski (1995).

[11] Note that the large error of our R_t estimate is due to a mild spatial extrapolation of the Stetson et al. (2003) data.

extended by including the Sauron database of ellipticals with available *GALEX* UV photometry, as discussed by Bureau et al. (2011; 41 galaxies, whose 5 objects in common with Buzzoni & González-Lópezlira 2008).

A more effective evolutionary characterization of the whole galaxy sample can be made by contrasting the $(1550-V)$ color with the Hβ equivalent width, as probed by the corresponding Lick index. Being especially sensitive to A-F stars (Gorgas et al. 1993; Buzzoni 1995a; Buzzoni et al. 2009), Hβ is an effective tracer of the turnoff temperature in the c-m diagram of intermediate-age (a few Gyr or so) stellar populations. A stronger Hβ absorption, combined with enhanced UV luminosity, is therefore an unequivocal sign of moderate but recent star formation activity in a galaxy, while a shallower feature always points to the presence of an underlying old (quiescent) stellar population.

The ">"-shaped trend of the galaxies in Figure 7 actually summarizes the general picture with a clear sequence of star-forming ellipticals (i.e., NGC 3032, 3156, 4150, etc., see, e.g., Temi et al. 2009, for a discussion) that diagonally cross the plot with decreasing Hβ and $(1550-V)$ and end in the lower right corner with the relevant case of NGC 1316 (a fresh post-merger object, see, e.g., Goudfrooij et al. 2001) and M32. By further decreasing the Balmer index (roughly for H$\beta \lesssim 2$ Å), one sees that the UV upturn begins to take shape especially for the group of giant ellipticals, namely NGC 4552, 4486, 1399, and 4649, characterized by an increasingly "blue" $(1550-V)$ color. In this framework, no doubt the case of NGC 6791 fits well with the quiescent ellipticals with the strongest UV upturn, although one has to note the slightly larger Hβ, in consequence of the relatively younger age of the cluster compared to the galaxy stellar populations.

Assuming the UV slope does not vary much among ellipticals, one can rely on the case of NGC 6791 to set a scale relationship between the $(1550-V)$ color, and the relative strength of galaxy UV emission, compared to the global bolometric luminosity. According to the color definition and relying on the figures of Table 1, we simply obtain[12]

$$\frac{L^{\rm UV}}{L^{\rm bol}_{\rm gal}} = 0.16 \times 10^{-0.4\,(1550-V)}. \qquad (7)$$

According to the galaxy distribution of Figure 7, UV-upturn ellipticals are expected to emit between 1% and 2.5% of their bolometric luminosity in the ultraviolet.

A more general view of the stellar bulk of NGC 6791 can be gained in the domain of classical broadband colors. A comparison with standard ellipticals is proposed in Table 1, after compiling Johnson and Cousins/Gunn mean colors from the original works of Yoshii & Takahara (1988) and Fukugita et al. (1995), respectively. We also took advantage of Hamilton's (1985) analysis of the $D4000$ Balmer-break index in the local and cosmological framework to derive a mean representative value of the index for present-day ellipticals (see Table 2 therein). This is reported in Table 1 as well, together with its observed standard deviation.

The UV-upturn feature is quantified in the table from the data of Figure 7 by averaging the $(1550-V)_o$ color of the four most UV-enhanced ellipticals in the plot, namely NGC 1399, 4486, 4552, and 4649. For these galaxies we also assumed a

[12] A similar relation can also be derived for the *GALEX* (FUV $-$ V) color such as $(L^{\rm UV}/L^{\rm bol}_{\rm gal}) = 2.06 \times 10^{-0.4\,({\rm FUV}-V)}$.

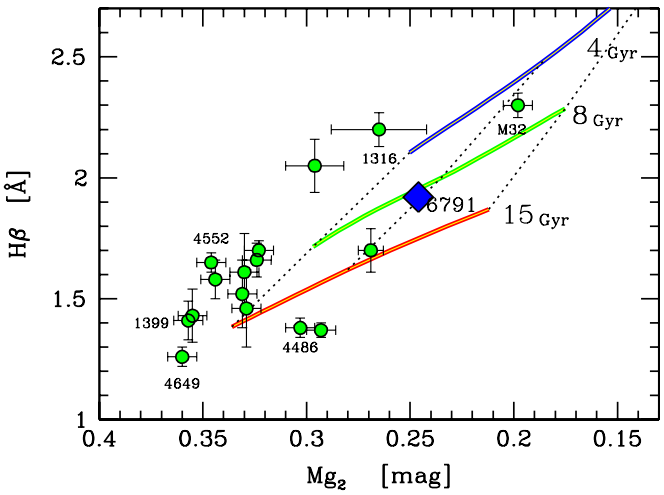

Figure 8. Buzzoni & González-Lópezlira (2008) compiled sample of elliptical galaxies displayed in the classical diagnostic plane of the Hβ vs. Mg_2 Lick indices, together with the corresponding location for NGC 6791 (big rhombus marker). Observations are compared with the Buzzoni (1989, 1995a) population synthesis models (with $Y = 0.25$) for an age of 4, 8, and 15 Gyr as labeled (solid lines), and for a metallicity parameter [Fe/H] $= -0.5$, 0.0, and +0.5, in the sense of increasing Mg_2 (dotted line envelope). In spite of its recognized value of [Fe/H] $\sim +0.4$, NGC 6791 appears here to match only a marginally supersolar metallicity due to its relatively low value of Mg_2. This is a consequence of the scanty population of RGB+AGB stars, a feature that we may ascribe to the speeded-up RGB evolution induced by helium overabundance. See the text for a discussion.

(A color version of this figure is available in the online journal.)

GALEX color (FUV $-$ NUV) $= 0.39$ from the reference SED of Buzzoni & González-Lópezlira (2008). According to Yi et al. (2011), only some 5% of present-day early-type galaxies actually display the UV-upturn phenomenon. For this reason, our figures in Table 1 should be taken as lower limits to the allowed color range for standard ellipticals in the local universe.

As far as optical colors are concerned, we see that NGC 6791 strictly matches the photometric properties of standard ellipticals. A systematic difference begins to appear, on the contrary, when moving to a longer wavelength in the near-infrared with increasingly brighter JHK magnitudes relative to the V luminosity ("redder" colors) for ellipticals with respect to the open cluster. An interesting difference can also be noticed for the 4000 Å Balmer jump, which is significantly shallower for the cluster with respect to the average elliptical. When specifically contrasted with UV-upturn galaxies, like NGC 4552 ($D4000 = 2.30$) and NGC 4486 ($D4000 = 2.06$), we see from Hamilton (1985) that in any case galaxy $D4000$ index exceeds the NGC 6791 estimate. As the $D4000$ feature mainly collects the photometric properties of the turnoff stars, increasing in value along the early- and late-type spectral sequence (see the instructive Figure 6 of Hamilton 1985), we are inclined to interpret this difference as a sign of the younger age of NGC 6791.

Finally, a comparison of the two most popular Lick indices, namely Hβ and Mg_2, is attempted in Figure 8. As is well known (Buzzoni 1995a, 1995b), this combination allows a simple and quite effective "taxonomy" of the H-R diagram of a stellar population because, while Hβ strength probes the turnoff location of the population (and therefrom its age), the integrated Mg_2 index better responds to the AGB+RGB contribution. When compared to its location in Figure 7, NGC 6791 moves now in the Lick plane toward the region of low-mass

metal-poorer ellipticals, like M32. When matched with standard population synthesis models (e.g., Buzzoni 1989, 1995a) the Hβ strength consistently confirms for the cluster an age about 8 Gyr, while Mg_2 points to just a marginally supersolar metallicity. According to our discussion in Section 3.1, this behavior may be the natural effect of a larger R parameter, as induced by an enhanced helium abundance. A coarser number of bright RGB+AGB stars would in fact reduce the integrated Mg_2 index and could also give reasons for the sensibly "bluer" infrared colors, thus mimicking the effect of a lower metallicity.

6. IMPLIED STELLAR LIFETIMES

Star number counts across our resolved H-R diagram of NGC 6791 can also be used to infer the absolute lifetime of the different post-main-sequence (PMS) evolutionary stages. This can be done by relying on the so-called FCT (Renzini & Buzzoni 1986), which, for every "jth" PMS phase, allows us to probe its implied lifetime (τ_j) just in terms of the number (n_j) of observed stars that currently sample it in the cluster diagram. Following Renzini & Buzzoni (1986), once accounting for the total collected luminosity of NGC 6791, we can write

$$n(j) = \mathcal{B}\, L_{6791}^{\rm bol}\, \tau(j). \quad (8)$$

In the equation, the parameter $\mathcal{B}$ is the so-called specific evolutionary flux and, according to stellar population synthesis models (see, e.g., Buzzoni 1989; Maraston 1998), it can safely be set to $\mathcal{B} \sim 2 \times 10^{-11}\ L_\odot^{-1}{\rm yr}^{-1}$. By recalling Equation (5), we eventually obtain

$$\tau(j) \simeq 2.0 \times 10^6\, n(j) \quad [{\rm yr}]. \quad (9)$$

In our sample one has therefore to expect, on average, one star per PMS evolutionary step of 2 Myr. Star number counts have been carried out for the NGC 6791 stellar population according to the scheme of Figure 9. Our results are summarized in Column 2 of Table 3 together with the implied lifetime (Column 3), as from Equation (9).

Although within the large uncertainties due to the low statistics, a close inspection of our data and a match with the several c-m diagrams available in the literature (see, in particular, Liebert et al. 1994 on this subject) allows us a preliminary estimate of the Iben (1968) R parameter to probe the helium content of the NGC 6791 stellar population. More properly, as a variant in case one cannot firmly discriminate between AGB and bright RGB stars, an alternative parameter $R' = N_{\rm HB}/N_{\rm GB}$ can also be tried, where $N_{\rm HB} = N_{\rm EHB} + N_{\rm RHB}$ and $N_{\rm GB} = N_{\rm BRGB} + N_{\rm AGB}$ includes both the RGB tail brighter than the red horizontal branch (RHB) luminosity level, and the AGB contribution. According to Table 3, we have $R' = 57/35 = 1.63 \pm 0.50$, where the error bar comes from a logarithmic differentiation, so that $dR'/R' \sim dN_{\rm HB}/N_{\rm HB} + dN_{\rm GB}/N_{\rm GB}$.

By relying on the Buzzoni et al. (1983) calibration, one may eventually figure out a helium abundance for the cluster of $Y_{6791} = 0.30 \pm 0.04$, in close agreement with the results of Brogaard et al. (2011) based on high-resolution spectroscopy of detached eclipsing binaries. This implies an enrichment ratio $\Delta Y/\Delta Z \sim 2$.

Although moving from opposite physical arguments, our picture may actually complement the original interpretative scheme proposed by Kalirai et al. (2007), as we have been anticipating in Section 3.1. Both the effect of enhanced mass loss and helium abundance act, in fact, in the sense of increasing the M_c/M_e ratio of PMS stars either by decreasing the envelope size (mass loss) or by increasing the He core mass (He overabundance). An enhanced M_c/M_e ratio favors post-RGB stars to anticipate their pathway to the WD final stage, in some cases by directly relocating in the high-temperature region of the H-R diagram both in the form of EHB or "hot flasher" stars (D'Cruz et al. 1996; Castellani et al. 2006a; Miller Bertolami et al. 2008; Yaron et al. 2008). Besides their synergic behavior to produce hotter HB stars, one major difference between the two evolutionary scenarios is that, contrary to mass loss, a change in helium abundance directly acts on the evolutionary lifetime as it affects the nuclear clock of stars along the whole He-burning phase.

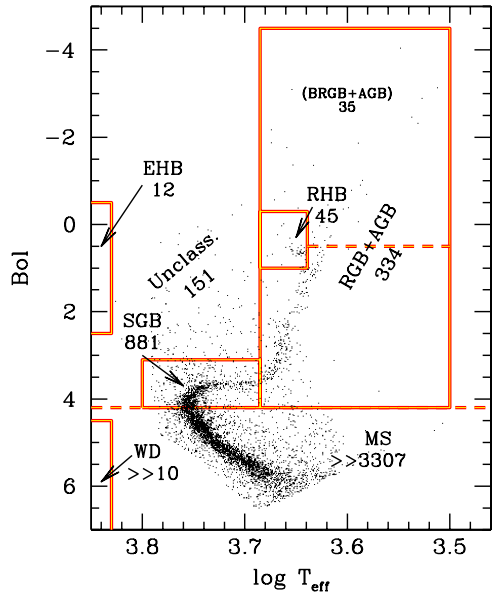

Figure 9. Zoomed-in sketch of the cluster H-R diagram with the selection scheme to pick up stars in the different evolutionary stages. The relevant star number counts (proportional to the evolutionary lifetime for PMS stars, according to Equation (9)) are reported in the different boxes, as summarized in better detail in Table 3.

(A color version of this figure is available in the online journal.)

A useful comparison of our output can be done with predictions from stellar evolution theory. Again, for this match we relied on the two reference sets of stellar tracks from the Basti (Pietrinferni et al. 2004) and Padova (Bertelli et al. 2008) databases assuming a very similar (solar-scaled) chemical composition, namely $(Z, Y) = (0.04, 0.30)$ for the Basti models and $(Z, Y) = (0.04, 0.34)$ for the corresponding Padova ones. Considering cluster age and chemical composition, a turnoff stellar mass of $M_{\rm TO} \simeq 1.1\ M_\odot$ has to be expected. This value is also consistent with the direct estimate of the primary stellar component of the detached binary system V20, almost exactly placed at the turnoff point and for which Grundahl et al. (2008) indicate a mass of $1.074\ M_\odot$. The resulting theoretical lifetime for PMS evolution is displayed in Columns 4 and 5 of Table 3.

In addition, we also added to the table (see Column 6) the relative bolometric contribution to cluster luminosity as from the observed stars in the different evolutionary stages. This ratio is actually the essence of the FCT and gives a direct hint of the nuclear fuel consumed by stars along their PMS evolution. By simply rearranging Equation (8) we can write

$$(n\,\overline{\ell})_j = \mathcal{B}\, L_{\rm tot}\, (\tau\,\overline{\ell})_j, \quad (10)$$

Table 3
Star Number Counts across the H-R Diagram of NGC 6791 and Implied Stellar Lifetime and Fuel Consumption

Stage	Number of Stars	Implied Lifetime	Theoretical Lifetime		$L_j/L_{\rm tot}$	H-equivalent Fuel ($M_\odot$)
			Basti	Padova		
MS	$\gg$3307	...	...	...	0.10	...
SGB	881	1762 ± 59 Myr	2390 Myr	1660 Myr	0.08	0.039 ± 0.001
RGB+AGB	333	666 ± 37 Myr	735 Myr	633 Myr	0.64	0.304 ± 0.017
RHB+EHB	45+12	114 ± 15 Myr	107 Myr	113 Myr	0.10	0.047 ± 0.006
WD	$\gg$10	...	...	...	0.00	...
Unclass.	151	...	...	...	0.08	0.040 ± 0.003
Total	4739				1.00	0.43 $M_\odot$±0.01
BRGB +AGB	35	70 ± 12 Myr	67 Myr	59 Myr		
R' =	57/35	1.63 ± 0.50	1.60 (Y = 0.30)	1.92 (Y = 0.34)		

where $\overline{\ell}(j)$ is the mean reference luminosity of stars along their jth evolutionary phase. This phase will provide a total emission $L_j = (n\,\overline{\ell})_j$ and a relative contribution to the global cluster luminosity of

$$\frac{L_j}{L_{\rm tot}} = \mathcal{B}\,\mathcal{F}_j. \qquad (11)$$

In the equation, $\mathcal{F}_j = (\tau\,\overline{\ell})_j$ is the fuel consumed by a star along its jth PMS evolutionary stage. After appropriate conversion (see Buzzoni 2011 for the detailed procedure) this figure can also be expressed in H-equivalent $M_\odot$, as reported in Column 7 of Table 3 (see also Renzini & Fusi Pecci 1988 and Maraston 1998 for an instructive application of this approach to other Galactic globular clusters).

A few interesting considerations stem from the combined analysis of the table entries. The first, and possibly most important one, deals with the implied HB lifetime. As far as the number counts are concerned, one sees from the table that a full score, including both the RHB and the EHB stars, is required to consistently compare with the theoretical expectations from both the Basti and Padova stellar tracks. This confirms therefore that both RHB and EHB stars are part of the *same* physical stage along the evolutionary path. According to our data, the HB phase for NGC 6791 stars lasts a total of $(45+12)\times 2 = 114 \pm 15$ Myr in close agreement with the theory. Along this phase, stars burn a total of $0.047 \pm 0.006\ M_\odot^H$, an output that has to be compared with the theoretical fuel figures of $0.041\ M_\odot^H$ and $0.057\ M_\odot^H$ for the Basti and Padova stellar tracks, respectively. Concerning the claimed presence of a few (∼10) supplementary HB stars at intermediate temperature filling the gap between the RHB clump and the EHB group, as suggested by Platais et al. (2011) but never confirmed before, this result seems unlikely as the implied HB lifetime could be hardly explained in terms of standard theory of stellar evolution.

While the energetic arguments about fuel consumption successfully account for star counts and the implied stellar lifetime, they can hardly explain the peculiar HB morphology as observed in NGC 6791, a striking sign of mass bimodality among HB stars. Other intervening mechanisms should likely be invoked in this sense to modulate HB morphology, perhaps through an "outside-in" action on the stellar envelope (thus leaving untouched the stellar clock), for instance, as a consequence of binary mass transfer (Yong & Demarque 2000; Yi & Yoon 2004).

As for the bright RGB (BRGB) evolution, models agree in predicting that stars complete their run from the HB luminosity level up to the RGB tip in about 51 Myr (Basti) or 42 Myr (Padova). If one adds a further 16–17 Myr for stars to accomplish their AGB evolution, then, according to Equation (9), a total of 30–35 bright stars are to be expected in our sample in fairly good agreement with what we observed. According to Table 3, the total "fuel" consumed by stars along their full RGB+AGB path amounts to $0.30 \pm 0.02\ M_\odot^H$, which is close to the corresponding theoretical figure of $0.25\ M_\odot^H$, as confirmed both by the Basti and Padova models. Enforced by our previous arguments about the R' ratio, this evidence points again to a relatively "quiescent" evolutionary scenario for NGC 6791, where the apparent deficiency in bright red giants seems a natural consequence of the enhanced helium abundance rather than of any harassing effect of mass loss via enhanced stellar wind. This argument is further supported by the results of van Loon et al. (2008), based on *Spitzer* observations, who find a definite lack of evidence for any circumstellar dust production that would accompany, in case, enhanced mass loss.

On the other hand, the Kalirai et al.'s (2007) unescapable evidence for $0.43\ M_\odot$ WDs in the cluster evidently suggests that *another* mechanism must be at work providing an efficient and alternative way for stars to loose mass. As a further piece of evidence on this line, one may also recall the recent works of Bedin et al. (2008) and Twarog et al. (2011), where a similar figure (namely ∼30% ± 10%) is independently found for the fraction of binary stars in NGC 6791. Further evidence for unresolved (close) binary systems among RHB stars has also been provided by Stello et al. (2011), based on asteroseismology observations from the *Kepler* space mission. According to Bedin et al. (2008), such a sizable component of binary systems may actually account for the observed WD peculiar distribution.

According to Figure 9, about 3% of our total bona fide sample (151 stars) cannot easily be arranged in our classification scheme. They provide 8% of our estimated cluster luminosity. If simply neglected, as in the most drastic interpretation that supposes all interlopers to be spurious, then we should decrease $L_{6791}^{\rm bol}$ accordingly, and this would lead to a correspondingly higher (+8%) implied PMS lifetime through Equation (8). Therefore, our estimates in Table 3 should be taken, in case, as lower limits.

A thorough assessment of membership probability in this region of the H-R diagram (see Platais et al. 2011) may actually lead us to envisage a certain fraction of field stars. However, one could argue that the evident overdensity of faint stars (some 30 objects, just above the turnoff region about $M_{\rm bol} \sim +3$) is certainly to be ascribed to the sizable population of cluster Blue Stragglers as extensively recognized in other literature studies (Kaluzny & Udalski 1992; Rucinski et al. 1996; Landsman et al.

1998; Kalirai et al. 2007). Ahumada & Lapasset (2007), in their revised catalog, report 75 blue straggler candidates for this cluster.

If fully considered in the cluster budget, according to the FCT the 151 "unclassified" stars would imply a supplementary fuel consumption of roughly 0.04 $M_{\odot}^{H}$. Therefore, a total of 0.43 $M_{\odot}$ of hydrogen (mainly converted to helium and some metals) has been consumed by NGC 6791 stars along their PMS evolution. Interestingly enough, this figure is very close to the Kalirai et al. (2007) estimate of WD mass, so that one may conclude that cluster stars reach the end of their PMS path after having fully exhausted (or lost) their external envelope.

A final consideration deals with the MS contribution, which in our sample amounts to a scanty 10% of the total cluster luminosity. This evidently has to be regarded as a lower limit, being that the faint red dwarf stars are beyond the limit of our detection.[13] Enforced by the discussion in Section 4 (see, in particular, Figure 6 therein), one could set a quite safe upper limit to the MS luminosity contribution such as $L_{\rm MS}/L_{\rm tot} < 0.20$. With this figure, however, even a quick check with the theoretical predictions from stellar population synthesis (Buzzoni 1989, 1995a) firmly points to a dwarf-depleted initial mass function (IMF; that is, with a slope consistent or flatter than the Salpeter case) for cluster stars.

7. SUMMARY AND CONCLUSIONS

In this work, we have carried out an analysis of the distinctive evolutionary properties of the stellar population in the old metal-rich Galactic open cluster NGC 6791. Our discussion moves from a set of original *UB* observations, which sampled the cluster field down to $B \sim 22$ mag. Lacking any systematic membership parameters for our stars, a statistical cleaning of the field interlopers across the cluster region has been adopted through an appropriate magnitude/color selection in the observed B versus $(U-B)$ c-m diagram as sketched in Figure 1. To better probe the few bright red giants in the cluster, we complemented our *UB* sample with the 2MASS *JK* output on the same field. The merged database of bona fide cluster stars brighter than $B = 21.5$ eventually consisted of 4739 objects.

Based on the UVBLUE theoretical library of synthetic stellar spectra from Rodríguez-Merino et al. (2005), we then derived a grid of calibrating relations for [Fe/H] = +0.4 so as to link the $(U-B)$ color with the effective temperature and the B-band bolometric correction (see Figure 2). This allowed us to estimate the fundamental parameters (namely $\log L$, $\log T_{\rm eff}$, and $\log g$) for 4706 available stars with accurate $(U-B)$ color, assuming a color excess $E(B-V) = 0.125$ and a distance modulus $(m-M)_o = 13.07$ after Twarog et al. (2009). A similar approach has also been carried out for the 94 2MASS stars relying on their $(J-K)$ color, through the Buzzoni et al. (2010) empirical calibration, as in Equation (4). The 61 stars of the 2MASS sample in common with the *UB* database allowed us to assess the internal accuracy of our calibration procedure. Accordingly, we concluded that effective temperature and bolometric luminosity have been retrieved, respectively, within a $\Delta \log T_{\rm eff} \simeq 0.03$ dex and ΔBol $\simeq$ 0.2 mag uncertainty. As a final output of our procedure, the H-R diagram of the cluster was obtained. This is shown in Figure 3 and has been the main reference for our investigation. The upper MS of the diagram is well matched by the PADOVA isochrones of Bertelli et al. (2008) for $t \simeq 7 \pm 1$ Gyr, assuming a $(Z, Y) = (0.04, 0.34)$ chemical mix. The turnoff point appears to be placed at $M_o^{\rm bol} = 4.2 \pm 0.2$, with an effective temperature $T_{\rm eff} \simeq 5700 \pm 50$ K, consistent with a spectral type G5V (Johnson 1966).

According to the fiducial $\log L$, $\log T_{\rm eff}$, and $\log g$ parameters, we attached to each star in our sample the appropriate synthetic spectrum, eventually obtaining the integrated SED of the cluster. In particular, high-resolution (2 Å FWHM) spectral synthesis has been carried out for the ultraviolet wavelength region, relying on the UVBLUE models, while its extension to a longer wavelength was accomplished at lower resolution by means of the Buzzoni (1989) synthesis code, which makes use of Kurucz's (1993) ATLAS9 grid of model atmospheres (see Figure 5). As a main output of our synthesis procedure, integrated cluster magnitudes and broadband colors both in the Johnson/Cousins and Gunn systems have been obtained, as summarized in Table 1. Furthermore, the full set of Fanelli et al. (1990) mid-UV narrowband indices was computed from the high-resolution SED. These have been complemented with a supplementary set of indices to assess the 4000 Å Balmer break (Brodie & Hanes 1986; Bruzual 1983) and the strength of the main spectral features in the optical range comprised in the Lick narrowband index system (Worthey et al. 1994; see Table 2). The sum of all the stars in our sample yields a total bolometric magnitude of $M_{6791}^{\rm bol} = -6.29$ or $L_{6791}^{\rm bol} = 25,350\, L_{\odot}$. A residual 15% luminosity fraction, at most, may have been lost in our census residing into the faintest undetected low-MS stars (see Figure 6). The corresponding figure for the V band is $M_{6791}^{V} = -5.60$, or 14,300 V solar luminosities, assuming from Portinari et al. (2004) $M_{\odot}^{V} = +4.79$.

As far as integrated cluster colors are concerned, according to Table 1, we obtain $(B-V)_{6791} = 0.97$ in fairly good agreement with Kinman's (1965) original estimate, and with a direct empirical check by summing up stars in the Kaluzny & Rucinski (1995) and Stetson et al. (2003) photometric catalogs, once picking up a cluster locus according to our selection criteria. When compared with the color properties of standard ellipticals (Yoshii & Takahara 1988; Fukugita et al. 1995; see Table 1), NGC 6791 appears to be a fairly good proxy. On closer analysis, however, one has to note significantly bluer infrared colors for the cluster, and a lower Mg_2 index. All these features are clearly reminiscent of a weaker photometric contribution of red giant stars in our system. The younger age of NGC 6791, compared to standard elliptical galaxies, also reflects in a slightly stronger Hβ absorption and a shallower 4000 Å Balmer break, as reported in Table 2 (see also Figure 8).

The UV properties of the integrated SED have been assessed both in terms of the classical $(1550-V)$ color, as originally defined by Burstein et al. (1988), and the updated $(\mathrm{FUV}-V)$ and $(\mathrm{NUV}-V)$ AB colors to match the *GALEX* photometric system. Once compared with extragalactic observations of elliptical galaxies, NGC 6791 appears to share the UV properties of the most active UV-upturn ellipticals, like NGC 4552 and NGC 4486 (see Figure 7), with a fraction of 1.7% ± 0.4% of its bolometric luminosity emitted in the ultraviolet wavelength range, shortward of 2500 Å (see Figure 5). This contribution is selectively supplied by the few stars hotter than ∼10,000 K. In particular, 12 stars may have been detected during their hot-HB evolution, in the form of EHB objects. While nine of them are known targets already classified by Kaluzny & Udalski (1992),

[13] Note, by the way, that part of the faintest undetected population of MS stars in the cluster may in fact already be accounted for in our photometry via blending effects with brighter objects. This would actually make "detected" stars slightly brighter and redder. A hint in this sense is for instance the drift toward "cooler" temperatures in the faint-end MS locus of Figure 3 when compared with theoretical isochrones.

three more stars are recognized in our field, being consistent with this scenario (see Paper II for further discussion). Coupled with the $(1550 - V)$ color—or its $(FUV - V)$ equivalent—the Hβ index is found to provide a simple and effective diagnostic tool to probe the nature of the UV excess in unresolved stellar systems. A "bluer" $(1550 - V)$ color, as in moderately star-forming ellipticals, for instance, will always accompany an enhanced Hβ absorption (indicatively, H$\beta \geqslant 2.0$ Å). The UV-upturn best candidates, therefore, stand out for their relatively lower Hβ, a definite sign of quiescent evolution.

A comparison with the D'Cruz et al. (1996) theoretical stellar tracks indicates that the hot edge of the HB stellar distribution in Figure 3 consistently agrees with the evolutionary track of a 0.45 $M_\odot$ star. Accordingly, most of the Kaluzny & Udalski (1992) stars currently seem at the limiting mass to ignite helium in their core (Dorman et al. 1995), and they may be evolving to the WD cooling sequence as AGB-*manqué* objects (Greggio & Renzini 1990; see, again, Figure 3). Quite interestingly, our arguments support the claimed evidence of Kalirai et al. (2007) for a prevailing fraction of He-rich low-mass stars with $M \sim 0.43 \pm 0.06\, M_\odot$ in the WD population of NGC 6791. Compared with the expected stellar mass at the turnoff point (about 1.07 $M_\odot$, according to Grundahl et al. 2008), such a reduced WD mass range evidently calls for an efficient and pervasive mechanism of mass loss along the PMS evolution. While stellar wind may obviously play a role, a combined series of arguments in our analysis may rather lead us to prefer an alternative scenario, where mass transfer mechanisms dealing with binary-system evolution might likely provide a viable channel to let the stellar envelope vanish along the full PMS evolutionary path (Carraro & Chiosi 1995; Carraro et al. 1996). One point in this sense is certainly the high $(30\% \pm 10\%)$ fraction of binary stars in the cluster (Bedin et al. 2008) and, at the same time, the lack of any explicit effect of enhanced stellar wind along red giant evolution (van Loon et al. 2008; Miglio et al. 2012). Rather than calling for any sort of "superwind" peeling-off process, as the analysis of Kalirai et al. (2007) may, for instance, lead one to envisage, the recognized evidence of a reduced lifetime and a correspondingly scanty population of RGB+AGB stars could more naturally be in consequence of a helium-rich chemical mix for the cluster stellar population. By relying on the Iben (1968) R' parameter, in fact, red giant number counts are consistent with $Y_{6791} = 0.30 \pm 0.04$, where the upper limit of the allowed range could be preferred considering the higher statistical probability for the few bright red giants to be field interlopers.

In this framework, it is interesting to remark on the excellent agreement between the implied lifetime of the different evolutionary branches in the cluster H-R diagram, as derived from the FCT theorem (Renzini & Buzzoni 1986), and the theoretical expectations from both the Padova (Bertelli et al. 2008) and Basti (Pietrinferni et al. 2004) stellar tracks, as summarized in Table 3. Both RHB and EHB stars are therefore to be considered as a part of the same evolutionary stage that physically coincides with the core He-burning phase and lasts in NGC 6791 a total of $t_{\rm HB} = 114 \pm 15$ Myr. One has to note, however, that the energetic arguments alone cannot explain the puzzling evidence that HB stars display this type of so-marked mass bimodality. Again, shocking "outside-in" physical mechanisms, possibly related to binary mass transfer, might be addressed to provide a more satisfactory solution in this sense (Yong & Demarque 2000; Yi & Yoon 2004). If this is the real case that applies to UV-enhanced ellipticals too, then one may be led to conclude that the UV-upturn phenomenon is a quite delicate result of tuned environment conditions (i.e., higher surface brightness and more "packed" stars) and evolutionary constraints (i.e., old and metal-rich stellar populations) inside galaxies. The marginal evidence for high-mass ellipticals to better display a UV excess in their SED is a clue in this sense (Burstein et al. 1988; Yi et al. 2011).

As the expected timescale for AGB completion turns about 16–17 Myr, according to the theoretical stellar tracks, then observations lead one to infer that the RGB alone has a total lifetime of $t_{\rm RGB} = 649 \pm 36$ Myr, with 53 ± 5 Myr spent at a brighter luminosity than the RHB clump. As for the MS properties, its reduced photometric contribution (just 10% of the total cluster luminosity in our sample) seems a firm result that is not substantially recovered even by accounting for lost faint stars, and rather points to an inherently dwarf-depleted IMF consistent or flatter than the Salpeter case.

In force of the FCT, by summing up the photometric contribution of stars along the different PMS phases, we derive from Table 3 a total fuel consumption of $0.43 \pm 0.01\, M_\odot$. This figure is in close agreement with the expected He core from theoretical tracks, and with the estimated WD mass of $\langle m_{\rm WD} \rangle = 0.43 \pm 0.06\, M_\odot$, indicating that cluster stars fully exhaust (or lose) their external envelope along the full PMS evolution. Such a tight agreement may also lead one to suspect, with Kalirai et al. (2007), that a fraction of the cluster stellar population does not reach the minimum mass required for stars to effectively ignite He in their cores.

One of us (A.B.) thanks the Instituto Nacional de Astrofisica Optica y Electronica of Puebla (Mexico) and the European Southern Observatory for generous financial support and warm hospitality during several visits to Mexico and at the ESO premises in Santiago de Chile, where part of this work was conceived. Partial financial support by Mexican SEP-CONACyT grant 47904 is also acknowledged.

This work has made use of different online galactic and extragalactic databases, including the Webda database for stellar clusters in the Galaxy and the Magellanic Clouds, maintained at the Institute of Astronomy of the University of Vienna, the Hyper-Linked Extragalactic Databases and Archives (HyperLeda) based at the Lyon University, and the VizieR catalog service of the Centre de Données astronomiques de Strasbourg.

REFERENCES

Ahumada, J. A., & Lapasset, E. 2007, A&A, 463, 789
Anthony-Twarog, B. J., Twarog, B. A., & Mayer, L. 2007, AJ, 133, 1585
Bedin, L. R., Piotto, G., Carraro, G., King, I. R., & Anderson, J. 2006, A&A, 460, L27
Bedin, L. R., Salaris, M., Piotto, G., et al. 2008, ApJ, 679, L29
Bertelli, G., Girardi, L., Marigo, P., & Nasi, E. 2008, A&A, 484, 815
Bertola, F., Bressan, A., Burstein, D., et al. 1995, ApJ, 438, 680
Bertola, F., Capaccioli, M., & Oke, J. B. 1982, ApJ, 254, 494
Boesgaard, A. M., Jensen, E. E. C., & Deliyannis, C. P. 2009, AJ, 137, 4949
Bressan, A., Chiosi, C., & Fagotto, F. 1994, ApJS, 94, 63
Brodie, J. P., & Hanes, D. A. 1986, ApJ, 300, 258
Brodie, J. P., & Huchra, J. P. 1990, ApJ, 362, 503
Brogaard, K., Bruntt, H., Grundahl, F., et al. 2011, A&A, 525, A2
Brown, T. M., Bowers, C. W., Kimble, R. A., Sweigart, A. V., & Ferguson, H. C. 2000, ApJ, 532, 308
Brown, T. M., Ferguson, H. C., Davidsen, A. F., & Dorman, B. 1997, ApJ, 482, 685
Brown, T. M., Ferguson, H. C., Stanford, S. A., & Deharveng, J.-M. 1998, ApJ, 504, 113
Bruzual, A. G. 1983, ApJ, 273, 105

Bureau, M., Jeong, H., Yi, S. K., et al. 2011, MNRAS, 414, 1887
Burstein, D., Bertola, F., Buson, L. M., Faber, S. M., & Lauer, T. R. 1988, ApJ, 328, 440
Buzzoni, A. 1989, ApJS, 71, 817
Buzzoni, A. 1995a, ApJS, 98, 69
Buzzoni, A. 1995b, in ASP Conf. Ser. 86, Fresh Views of Elliptical Galaxies, ed. A. Buzzoni, A. Renzini, & A. Serrano (San Francisco, CA: ASP), 189
Buzzoni, A. 2007, in ASP Conf. Ser. 375, From Stars to Galaxies: Building the Pieces to Build Up the Universe, ed. A. Vallenari et al. (San Francisco, CA: ASP), 311
Buzzoni, A. 2011, MNRAS, 415, 1155
Buzzoni, A., Battistini, C., Carrasco, L., & Recillas, E. 2009, Rev. Mex. Astron. Astrofis. Ser. Conf., 37, 110
Buzzoni, A., Fusi Pecci, F., Buonanno, R., & Corsi, C. E. 1983, A&A, 128, 94
Buzzoni, A., Gariboldi, G., & Mantegazza, L. 1992, AJ, 103, 1814
Buzzoni, A., & González-Lópezlira, R. A. 2008, ApJ, 686, 1007
Buzzoni, A., Mantegazza, L., & Gariboldi, G. 1994, AJ, 107, 513
Buzzoni, A., Patelli, L., Bellazzini, M., Pecci, F. F., & Oliva, E. 2010, MNRAS, 403, 1592
Carney, B. W., Lee, J.-W., & Dodson, B. 2005, AJ, 129, 656
Carraro, G., & Chiosi, C. 1995, IAA-IAC-University of Pisa Workshop, The Formation of the Milky Way, ed. E. J. Alfaro & A. J. Delgado (Cambridge: Cambridge Univ. Press), 175
Carraro, G., Girardi, L., Bressan, A., & Chiosi, C. 1996, A&A, 305, 849
Carraro, G., Girardi, L., & Chiosi, C. 1999, MNRAS, 309, 430
Carraro, G., Villanova, S., Demarque, P., et al. 2006, ApJ, 643, 1151
Castellani, M., Castellani, V., & Prada Moroni, P. G. 2006a, A&A, 457, 569
Castellani, V., Iannicola, G., Bono, G., et al. 2006b, A&A, 446, 569
Castelli, F., & Kurucz, R. L. 2003, in IAU Symp. 210, Modelling of Stellar Atmospheres, ed. N. Piskunov, W. W. Weiss, & D. F. Gray (San Francisco, CA: ASP), 210
Chaboyer, B., Green, E. M., & Liebert, J. 1999, AJ, 117, 1360
Chavez, M., Bertone, E., Buzzoni, A., et al. 2007, ApJ, 657, 1046
Code, A. D., & Welch, G. A. 1979, ApJ, 228, 95
Code, A. D., & Welch, G. A. 1982, ApJ, 256, 1
D'Cruz, N. L., Dorman, B., Rood, R. T., & O'Connell, R. W. 1996, ApJ, 466, 359
D'Cruz, N. L., Morgan, S. M., & Böhm-Vitense, E. 2000, AJ, 120, 990
Dorman, B., O'Connell, R. W., & Rood, R. T. 1995, ApJ, 442, 105
Fanelli, M. N., O'Connell, R. W., Burstein, D., & Wu, C.-C. 1990, ApJ, 364, 272
Fukugita, M., Shimasaku, K., & Ichikawa, T. 1995, PASP, 107, 945
Girardi, L., Groenewegen, M. A. T., Hatziminaoglou, E., & da Costa, L. 2005, A&A, 436, 895
Gorgas, J., Cardiel, N., Pedraz, S., & González, J. J. 1999, A&AS, 139, 29
Gorgas, J., Faber, S. M., Burstein, D., et al. 1993, ApJS, 86, 153
Goudfrooij, P., Alonso, M. V., Maraston, C., & Minniti, D. 2001, MNRAS, 328, 237
Gratton, R., Bragaglia, A., Carretta, E., & Tosi, M. 2006, ApJ, 642, 462
Greggio, L., & Renzini, A. 1990, ApJ, 364, 35
Grundahl, F., Clausen, J. V., Hardis, S., & Frandsen, S. 2008, A&A, 492, 171
Hamilton, D. 1985, ApJ, 297, 371
Harris, W. E. 1974, ApJ, 192, L161
Iben, I. 1968, Nature, 220, 143
Iben, I., Jr., & Renzini, A. 1983, ARA&A, 21, 271
Johnson, H. L. 1966, ARA&A, 4, 193
Kalirai, J. S., Bergeron, P., Hansen, B. M. S., et al. 2007, ApJ, 671, 748
Kaluzny, J., & Rucinski, S. M. 1995, A&AS, 114, 1
Kaluzny, J., & Udalski, A. 1992, Acta Astron., 42, 29
King, I. R. 1966, AJ, 71, 64
Kinman, T. D. 1965, ApJ, 142, 655
Kurucz, R. L. 1993, CD-ROM 13, Atlas9 Stellar Atmosphere Programs and 2 km/s Grid (Cambridge: Smithsonian Astrophys. Obs.)
Landolt, A. U. 1992, AJ, 104, 340
Landsman, W., Bohlin, R. C., Neff, S. G., et al. 1998, AJ, 116, 789
Lata, S., Pandey, A. K., Sagar, R., & Mohan, V. 2002, A&A, 388, 158
Liebert, J., Saffer, R. A., & Green, E. M. 1994, ApJ, 107, 1408
Maraston, C. 1998, MNRAS, 300, 872
Miglio, A., Brogaard, K., Stello, D., et al. 2012, MNRAS, 419, 2077
Miller Bertolami, M. M., Althaus, L. G., Unglaub, K., & Weiss, A. 2008, A&A, 491, 253
Montgomery, K. A., Janes, K. A., & Phelps, R. L. 1994, AJ, 108, 585
Neff, S. G., Hollis, J. E., & Offenberg, J. D. 2008, Galex Observer's Guide, web edition available online at http://galexgi.gsfc.nasa.gov/docs/galex/Documents
Origlia, L., Valenti, E., Rich, R. M., & Ferraro, F. R. 2006, ApJ, 646, 499
Paczyński, B. 1970, Acta Astron., 20, 47
Peterson, R. C., & Green, E. M. 1998, ApJ, 502, L39
Pietrinferni, A., Cassisi, S., Salaris, M., & Castelli, F. 2004, ApJ, 612, 168
Pietrinferni, A., Cassisi, S., Salaris, M., & Castelli, F. 2006, ApJ, 642, 797
Pietrinferni, A., Cassisi, S., Salaris, M., Cordier, D., & Castelli, F. 2007, in IAU Symp. 241, Stellar Populations as Building Blocks of Galaxies, ed. A. Vazdekis & R. F. Peletier (Cambridge: Cambridge Univ. Press), 39
Platais, I., Cudworth, K. M., Kozhurina-Platais, V., et al. 2011, ApJ, 733, L1
Portinari, L., Sommer-Larsen, J., & Tantalo, R. 2004, MNRAS, 347, 691
Renzini, A., & Buzzoni, A. 1986, in Spectral Evolution of Galaxies, ed. C. Chiosi & A. Renzini (Astrophysics and Space Science Library, Vol. 122; Dordrecht: Reidel), 195
Renzini, A., & Fusi Pecci, F. 1988, ARA&A, 26, 199
Rodríguez-Merino, L. H., Chavez, M., Bertone, E., & Buzzoni, A. 2005, ApJ, 626, 411
Rucinski, S. M., Kaluzny, J., & Hilditch, R. W. 1996, MNRAS, 282, 705
Skrutskie, M. F., Cutri, R. M., Stiening, R., et al. 2006, AJ, 131, 1163
Stello, D., Huber, D., Kallinger, T., et al. 2011, ApJ, 737, L10
Stetson, P. B. 1987, PASP, 99, 191
Stetson, P. B., Bruntt, H., & Grundahl, F. 2003, PASP, 115, 413
Temi, P., Brighenti, F., & Mathews, W. G. 2009, ApJ, 695, 1
Twarog, B. A., Anthony-Twarog, B. J., & Edgington-Giordano, F. 2009, PASP, 121, 1312
Twarog, B. A., Carraro, G., & Anthony-Twarog, B. J. 2011, ApJ, 727, L7
van Loon, J. T., Boyer, M. L., & McDonald, I. 2008, ApJ, 680, L49
Worthey, G., Faber, S. M., Gonzalez, J. J., & Burstein, D. 1994, ApJS, 94, 687
Wu, Z.-Y., Zhou, X., Ma, J., & Du, C.-H. 2009, MNRAS, 399, 2146
Xin, Y., & Deng, L. 2005, ApJ, 619, 824
Yaron, O., Kovetz, A., & Prialnik, D. 2008, in IAU Symp. 252, The Art of Modeling Stars in the 21st Century, ed. L. Deng & K. L. Chan (Cambridge: Cambridge Univ. Press), 261
Yi, S. K., Lee, J., Sheen, Y.-K., et al. 2011, ApJS, 195, 22
Yi, S. K., & Yoon, S.-J. 2004, Ap&SS, 291, 205
Yong, H., Demarque, P., & Yi, S. 2000, ApJ, 539, 928
Yoshii, Y., & Takahara, F. 1988, ApJ, 326, 1